

This document is downloaded from DR-NTU, Nanyang Technological University Library, Singapore.

Title	Highly stretchable and self-deformable alternating current electroluminescent devices
Author(s)	Wang, Jiangxin; Yan, Chaoyi; Chee, Kenji Jianzhi; Lee, Pooi See
Citation	Wang, J., Yan, C., Chee, K. J., & Lee, P. S. (2015). Highly stretchable and self-deformable alternating current electroluminescent devices. <i>Advanced materials</i> , 27(18), 2876-2882.
Date	2015
URL	<a href="http://hdl.handle.net/10220/25375">http://hdl.handle.net/10220/25375</a>
Rights	© 2015 Wiley-VCH Verlag GmbH & Co. KGaA, Weinheim. This is the author created version of a work that has been peer reviewed and accepted for publication by <i>Advanced materials</i> , Wiley-VCH Verlag GmbH & Co. KGaA, Weinheim. It incorporates referee's comments but changes resulting from the publishing process, such as copyediting, structural formatting, may not be reflected in this document. The published version is available at: [ <a href="http://dx.doi.org/10.1002/adma.201405486">http://dx.doi.org/10.1002/adma.201405486</a> ].

DOI: 10.1002/adma.((please add manuscript number))

**Article type: Communication****Highly stretchable and self-deformable alternating current electroluminescent devices***By Jiangxin Wang, Chaoyi Yan, Kenji Jianzhi Chee, and Pooi See Lee\**

J. X. Wang, Dr. C. Y. Yan, K. J. Chee, Prof. P. S. Lee

School of Materials Science and Engineering

50 Nanyang Avenue

Nanyang Technological University

Singapore, 639798

E-mail: pslee@ntu.edu.sg

K. J. Chee, Prof. P. S. Lee

Institute of Sports Research

Nanyang Technological University

Singapore 639798

Keywords: Stretchable light-emitting devices, self-deformable, alternating current

electroluminescent, actuator, nanowires

Emerging soft electronics which are mechanically deformable and malleable are pushing the boundaries of rigid devices. EL devices with good mechanical compliance can benefit and inspire a plethora of new applications such as deformable and stretchable displays, conformable visual readout on arbitrary shapes, biomedical imaging and monitoring devices *etc.* Previous stretchable EL devices were mainly demonstrated by research groups of Rogers,<sup>[1,2]</sup> Pei,<sup>[3-5]</sup> and Someya<sup>[6,7]</sup> either employing intrinsically stretchable materials or stretchable device structures. Challenges in the intrinsically stretchable luminescent devices persist in that their emission intensity significantly reduced under large strains and the device could not survive large strain cycles, while the devices employing stretchable structures meet difficulties in the complicated fabrication procedures and non-stretchable light-emitting elements. Moreover, all these pioneering works were geared toward developing EL devices with maintained device functionality while passively deformed by external force. We hereby report the fabrication of

intrinsically stretchable EL devices with ACEL materials via an all-solution processible method.

The stretchable EL device showed excellent stability under large strains and could maintained its good performance under large strain cycles. Furthermore, we demonstrate that the stretchable EL devices could be driven to dynamic shapes upon integration with electrical actuators. The novel functionality will offer new opportunities and dimensions in the soft electronics which are unreachable with conventional technologies. For example, volumetric displays which render 3D contents physically and are capable of providing users tactile interaction besides digital information presentation will offer an immersive display experience.<sup>[8-11]</sup> In retrospect, impressive applications have been demonstrated by the MIT's Tangible Media Group with the use of 2D linear actuator arrays.<sup>[8-11]</sup> However, their large and heavy mechanical actuation systems impede light weight and high resolution realization.

The development of mechanical "robust" EL devices, which can confront different demanding mechanical deformations such as flexing, folding, twisting and stretching without incurring damage, is the primary requirement for fabricating the self-deformable EL devices. Reported attempts have demonstrated polymer light-emitting materials for intrinsically stretchable EL devices.<sup>[3-7,12]</sup> Different strategies were also employed by engineering stretchable structures with assembled rigid inorganic light-emitting elements.<sup>[1,2,13,14]</sup> Substrates and electrodes of the devices can be stretched while the light-emitting elements were kept intact during stretching. Here, a different method was developed to fabricate intrinsically stretchable inorganic EL device with both stretchable conductors and light-emitting layers. The elastic EL device could sustain its performance at stretching strains as large as 100% (close to the mechanical failure of the host elastomer). Simplicity of the device fabrication together with their excellent stretchability enabled the integration with actuators which could drive the elastic EL devices into dynamic shapes. Dielectric elastomer actuators (DEAs) are emerging "smart materials" which can generate mechanical motions with applied electrical fields. DEAs have demonstrated

extraordinary mechanical actuation performance with area strain reaching beyond 200% on prestrained elastomer,<sup>[15-17]</sup> which exceeds most of the actuators based on other working mechanisms, such as piezoelectric actuators (~5%),<sup>[18]</sup> ionic gel actuators (~40%),<sup>[19]</sup> and natural muscle (~100%).<sup>[20]</sup> With their intrinsic stretchability, ease of minimization, high power density and low-cost fabrication, DEAs have been applied in many applications such as wearable tactile display devices,<sup>[21,22]</sup> high-speed electromechanical transducers,<sup>[23,24]</sup> and smart artificial muscles<sup>[20,25]</sup> *etc.* In this report, the DEAs are demonstrated to be ideal shape display components to integrate with the stretchable EL devices. An unprecedented self-deformable EL device is fabricated by the innovative method in this work.

A schematic drawing of the stretchable EL device is represented in Figure 1a. The stretchable EL device was fabricated with a simple all-solution processible method. In brief, AgNW networks were firstly spray-coated onto the Polydimethylsiloxane (PDMS) substrate, forming the bottom electrode. ZnS:Cu micro-particles mixed with liquid PDMS was then spun onto the bottom electrode. ACEL devices have been developed for display or lighting applications for a few decades and attracted persistent interest for their simple device architecture and low production cost.<sup>[26-28]</sup> ZnS:Cu is a widely available ACEL material with well studied and understood emission behavior.<sup>[29,30]</sup> Its emission colors can be easily tuned by using different active dopants or adjusting the dopant concentrations. After crosslinked, the ZnS:Cu/PDMS composite layer harvest the excellent stretchability from the PDMS matrix with sustained functionality of the emissive material. PDMS is quite stable against most of the solvents.<sup>[31]</sup> AgNWs dissolved in isopropyl alcohol (IPA) can be directly deposited onto the ZnS:Cu/PDMS composite without concern of solvent attack to the light-emitting layer. It should be noted that while solvent compatibility problem is hard to avoid in most organic EL devices, the stable property of the inorganic light-emitting layer provides great advantage to ease the device fabrication. Another thin PDMS was spin-coated after the top electrode deposition to embed the AgNW networks and cap the whole device structures. The capping layer constrained and

protected the AgNW network in the polymer matrix so that its conductivity can be maintained under stretching-releasing operations. The cross-linked PDMS significantly reduced the oxygen concentration surrounding the AgNWs,<sup>[32]</sup> protecting them from oxidation. In addition, the PDMS matrix isolated the device structure from moisture which might react with the EL phosphors and quench the luminescence. Schematic images of the luminous EL device are depicted in the right of Figure 1a. Benefited from its geometry design, the EL device is expected to maintain the functionality under large mechanical deformations such as stretching, flexing or twisting. Figure 1b (left) is a fabricated device with semitransparent appearance (the background can be seen through the EL device). The device was fabricated with transparent AgNW networks as the top and bottom electrodes. Consequently, light emission can be extracted from both sides of the device. The right image in Figure 1b shows the device powered by an AC bias with bright green emission. Structure simplicity in the ACEL device enables other modifications on the fabrication procedure to achieve different functionalities. For instance, as the emission wavelength from ZnS is determined primarily by the doping activators, ZnS:Mn and ZnS:Al particles can be used to produce emission in the red and blue colors, providing the other two primary colors for full-color image display applications. The EL device can also be easily patterned into row and column arrays to achieve independent addressing and control of individual pixel. Patterning the bottom electrodes of the stretchable EL devices was achieved in this report (supporting information [Figure S1](#)).

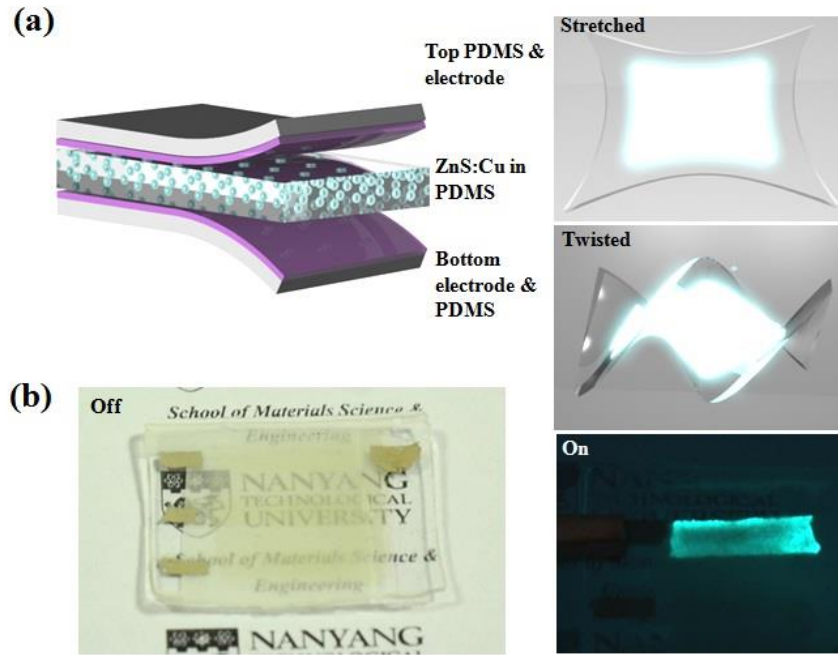


**Figure 1.** (a) Schematic images showing the device geometry (left) and the luminous EL device under mechanical manipulations of stretching and twisting (right). (b) Photographs of the fabricated device in the off state (left) and on state (right).

The AgNW percolating network coated on the crosslinked PDMS surface was examined and shown in Figure 2a. A homogenous and interconnecting network was obtained after the spray coating process, which was critical to achieve electrodes with good conductivity and transparency. The AgNWs have diameter of 120-150 nm and length of 20-50  $\mu\text{m}$ . Junction resistance is the dominant factor which affects the conductivity of the metallic network. The network structure can easily be displaced and lose its conductivity without constrain on the NW junctions during repeated stretching-releasing cycles.<sup>[33]</sup> Generally, elastic polymers were used to embed the conducting structures so that the nanowires could harvest the restoring force from the polymer matrix and maintain their locations in the host polymers under deformations. Instead of using the embedment and transfer method, the AgNW films were directly coated and simultaneously buried by the polymer matrix in subsequent layer deposition. Apart from delivering a simple and scalable process for fabrication, the method can avoid damage to the

conducting network during the transfer step which could induce significant conductivity degradation to the transparent electrodes.<sup>[34,35]</sup> Figure 2b shows the cross section of the AgNW film after embedded into the PDMS matrix. The SEM image shows that the top PDMS layer penetrates through the AgNW network and combines with the bottom PDMS substrate. The liquid PDMS partially dissolved the PDMS substrate at the interface during the solidification process, leading to “in situ” assembling of the different layers. The bonding strength at the interfaces was much stronger compared to other assembling methods such as hot-press lamination, oxygen plasma bonding, or corona discharge bonding *etc.*<sup>[36]</sup> The strong bonding force is crucial to maintain the device performance under different mechanical deformations as the interfaces are more vulnerable compared to other parts in the device during compressing, twisting, or flexing. Morphology of the ZnS:Cu particles are shown in Figure 2c, which have an average diameter of 29  $\mu\text{m}$ . Thickness of the light-emitting film ( $\sim 41 \mu\text{m}$ , Figure 2d) was mainly affected by the diameter of the particles during the spin-coating process. Roughness of the AgNW network is about 120 nm, characterized by an atomic force microscopy (AFM), supporting information Figure S2a. The roughness of the AgNW network is small compared to the thickness of the light-emitting layer, eliminating our concern that roughness of the AgNW network may induce device failure under high electrical field (supporting information Figure S2b).

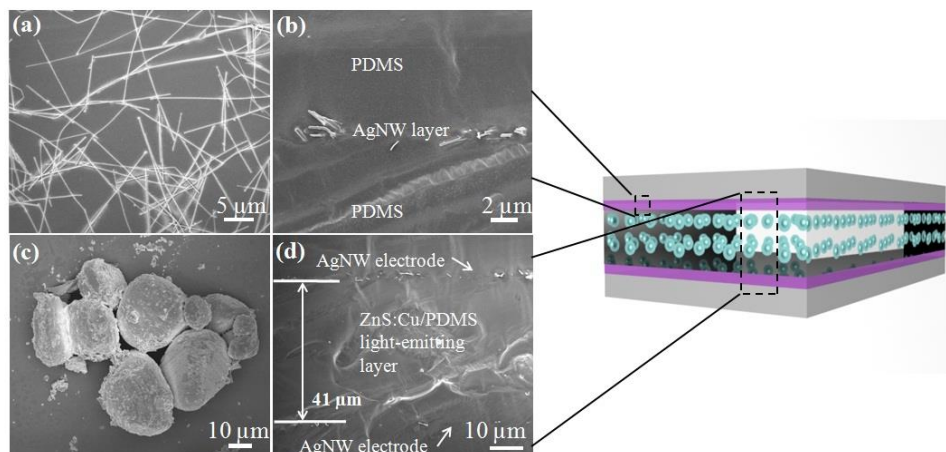


**Figure 2.** SEM characterization of the elastic EL device: (a) AgNWs sprayed-coated onto the PDMS substrate; (b) cross-section observation of the AgNWs after embedded into PDMS matrix; (c) morphology of the ZnS:Cu micro-particles; (d) cross-section observation of the device geometry.

The stretchable EL device was powered with a rectangular pulse function (pulse voltage of +/- 120 V, frequency of 2.5 kHz). The EL device demonstrated excellent mechanical compliant properties with all structures embedded and protected by the PDMS matrix. It could be bended 180° or folded face-to-face (Figure 3a) and twisted (Figure 3b). The device functionality was maintained and no degradation was observed during the mechanical deformation. The excellent mechanical compliant property exceeds conventional flexible EL devices. The device can be elongated to a stretching strain of 100% with maintained functionality before break down of the host polymer, as shown in Figure 3c. The EL emission spectrum was centered at 495 nm with FWHM (full-width-at-half-maximum) of 80 nm, as interpreted in Figure 3d (the commission international de l'Eclairage (CIE) color coordinate was shown in supporting information [Figure S3](#)). It is understood that under electrical field excitation, the charge carriers were accelerated into high energy. The hot carriers will cause excitation or ionization of the luminescent center, generating electron-hole pairs. Luminescence is produced as a result of the exciton relaxation through radiative recombination. Compared to the host lattices, dopants in ZnS typically demonstrate a more effective radiative recombination path for the excitons, evident by the photoluminescent (PL) spectrum (supporting information [Figure S4](#)) and EL emission spectrum. The emission intensity against the applied electrical field and voltage under different frequencies is plotted in Figure 3e. The device initiated light emission at the bias voltage of around 60 V after which the emission intensity increased rapidly. The relation between the bias voltages and EL intensity can be evaluated by the following equation:<sup>[37]</sup>

$$L=L_0\exp(-\beta/V^{1/2}) \quad (1)$$

where  $L$  is the luminance,  $V$  is the voltage,  $L_0$  and  $\beta$  are the constants decided by the devices.<sup>[38]</sup>

After a certain bias voltage, the probability of electrons to be accelerated to a given energy and excite (or ionize) subsequently the luminescent centers will increase steeply, corresponding to the rapid increase in the luminescent intensity. The fitting curve in Figure 3e shows that the experiment data agrees well with Equation 1. Discussion and performance of the device under higher voltage can also be found in the supporting information [Figure S2b](#). Stretchability of the EL device was tested by elongating the device to different strains under a stretching speed of 1 mm/s, corresponding to a strain rate of  $\sim 3\%/s$  with the original device length of 35 mm. The ACEL devices can also be stretched under higher speeds. Performance of the device under different stretching speeds is included in the supporting information [Figure S5](#). A video was also included in the supporting information to demonstrate the device manually stretched at different speeds. Stable light emission was sustained in the device with strain up to 100% as shown in Figure 3f. The emission intensity increased slightly by  $\sim 11\%$  of the initial intensity at the strain of 30%. Further increase in the stretching strain led to a small decrease in the emission intensity ( $\sim 13\%$  decrease at the stretching strain of 100%). The intensity change might be due to a combine effect of increase in the emission areas (corresponding to smaller density of the light-emitting particles) and decrease in the emission layer thickness (corresponding to larger electrical field on the light-emitting particles). Under smaller stretching strains, increase in the electrical field might contribute more to the increase in emission intensity while decrease in the particle density dominated at larger stretching strains. Previous report on EPLEDs<sup>[5]</sup> showed declining luminance under increased stretching strains ( $\sim 89\%$  decrease in the emission intensity at 100% strain compared to the initial intensity at 0% strain), which was attributed to the reduced injection current density. The stable performance of the elastic EL device here could be attributed to the good mechanical compliant property of the device architecture and the unique emission mechanism of ACEL devices. It is still difficult to avoid the large conductivity change of transparent AgNW networks under stretching strains ( $\Delta R/R_0 > 20$  at

stretching strain of 100%,  $\Delta R$  is the resistance increase and  $R_0$  is the origin resistance).<sup>[4,5,34]</sup>

However, the elastic ACEL device demonstrated in this work is capacitively coupled to the external electrical bias with small current. The emission intensity is mainly determined by the bias voltage ( $L=L_0\exp(-\beta/V^{1/2})$ ) instead of the conductive components of current.<sup>[39]</sup> The resistance change in the AgNW network under strains is still very small compared to the device resistance, leading to a stable performance in the EL device under stretching. The EL device was also subjected to repeated stretch and relaxation cycles, showing stable performance under the cycling test. Switching test of the EL device indicated that the device can be turned on and off promptly. Further evaluation on the device performance can be found in the supporting information [Figure S6](#).

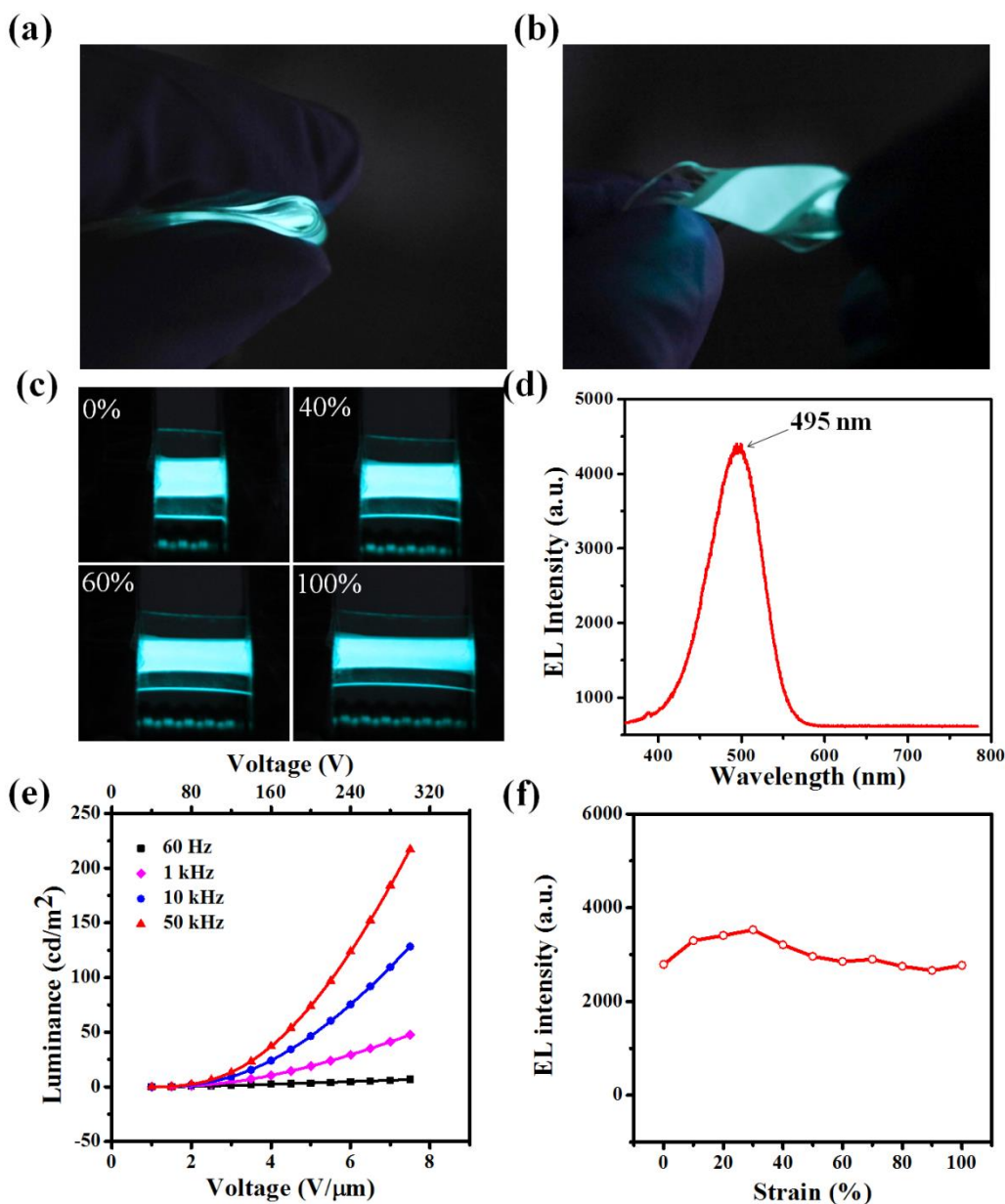


**Figure 3.** Photographs of the EL device (a) bended 180° or folded face-to-face; (b) twisted; (c) stretched to the strains of 0%, 40%, 60% and 100%. (d) Electroluminescent spectrum of the elastic EL device. (e) Luminance of the stretchable ACEL device under different frequencies and the fitting of luminance with the applied voltage. (f) Emission intensity change of the EL device under different stretching strains.

To achieve the self-deformable EL devices, the stretchable EL devices were fabricated on DEAs with the aforementioned processes. As shown in Figure 4a, the device fabrication started with a 3M VHB poly(acrylic) substrate prestrained biaxially to 300%. AgNWs were spray-coated

on both sides of the prestrained film, working as the top and bottom electrodes for the actuator. Compared to conventional electrodes such as powder carbon graphite and carbon black in grease, conductivity in the AgNW film is established by the network structure which helps to accommodate large stretching strains. Moreover, the highly conductive metallic NW network possess unique properties such as good transparency with high conductivity, thin structure with smaller impeding stiffness on the actuation and capability of self-clearing to prevent premature dielectric failure.<sup>[15]</sup> ZnS:Cu particles mixed with silicone was spun onto the top electrode as the light-emitting layers. Top electrode (spray-coated AgNWs) and silicone capping layer were deposited subsequently to complete the device fabrication. Figure 4b provides a cross-section view of the device structure.

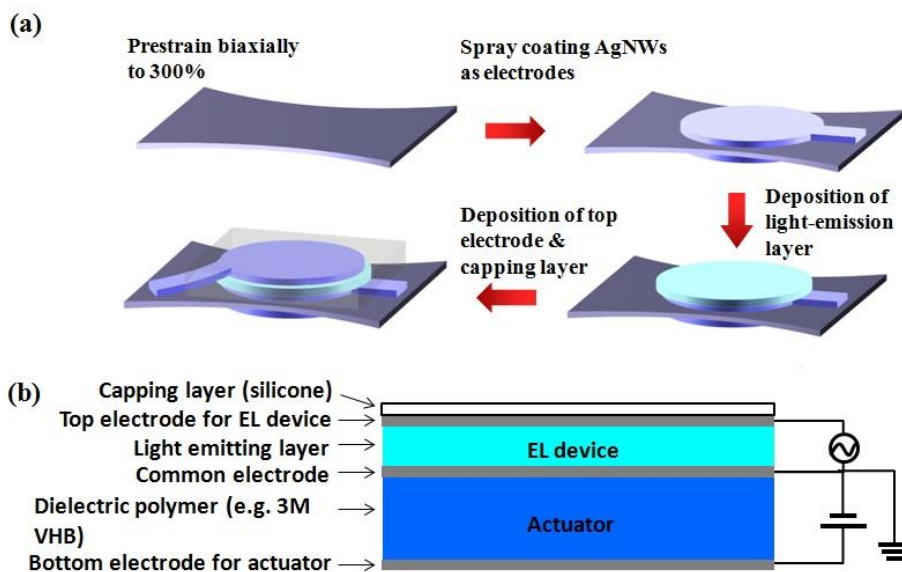


**Figure 4.** (a) A schematic interpreting the fabrication procedure of the actively self-deformable EL device. (b) Cross-section view of the device structure.

The electrical actuation performances were firstly examined after completing the DEA fabrication. Different amount of AgNWs were used for the electrode deposition. AgNWs with the concentration of 0.3 mg/ml was used while the solution volumes were varied from 1.5, 2 to 2.5 ml. DEA electrodes with the same dimension were coated on both side of the dielectric

elastomer. As shown in Figure 5a, increasing the AgNW solution resulted in an augmented area strain, where the area strain (%) is defined as  $[(\text{actuated area}) - (\text{unactuated area})] / (\text{unactuated area})$ . Under the electrical bias, opposite charges on the top and bottom electrodes of the actuator will generate attraction force while the similar charges on the same electrodes give repulsion force, causing the Maxwell stress ( $p = \epsilon \epsilon_0 E^2$ ,  $\epsilon$  is the relative permittivity of the elastomer,  $\epsilon_0$  is the permittivity of free space, and  $E$  is the applied electrical field) on the elastomer. The Maxwell stress compresses the elastomer along its thickness and causes it to expand laterally. The device with more AgNWs could maintain the conductivity at higher area expansion when the elastomer was actuated, leading to a better actuation performance. As can be seen in the photograph of Figure 5b, the actuator fabricated with 2.5 ml AgNWs solution showed area expansion of 67% at the voltage of 5 kV and increased above 106% at the voltage of 5.5 kV (buckling existed in the elastomer due to the silver paste on the edge of the NW electrodes, shown in the supporting information [Figure S7a](#), indicating that area expansion was undervalued). Under the same voltage of 5 kV, the area strain increased from ~54%, 72% to 106% with the increased solution volume from 1.5, 2 to 2.5 ml.

The stretchable EL devices were assembled with the DEAs using 2.5 ml AgNW solution for the electrode fabrication. Performance of the self-deformable EL device was examined and presented in Figure 5c. The EL device was powered with a rectangular pulse function (constant pulse voltage of +/- 120 V, frequency of 2.5 kHz) for light emission and the DEA was actuated under different bias voltages for shape changes. The area expansion increased with the ramping voltage. The EL device works stably under different strain states, as shown in Figure 5d. The increase trend of the device area is similar to the actuator before the EL device integration with reduced expansion magnitude (55% area strain at 5 kV compared to 67% area strain at 5 kV before integration). It can be attributed to the additional layers of the EL devices which hinder the actuation behavior. With the constant Maxwell stress under the same voltage, the area expansion is reciprocal to the device elastic modulus. The introduced elastic EL layer slightly

increased the elastic modulus of the whole devices, leading to the reduced area expansion under the same stress. Similarly to the actuator without EL layer, the integrated device showed buckling structure under higher actuating voltage, as shown in the supporting information

Figure S7b.

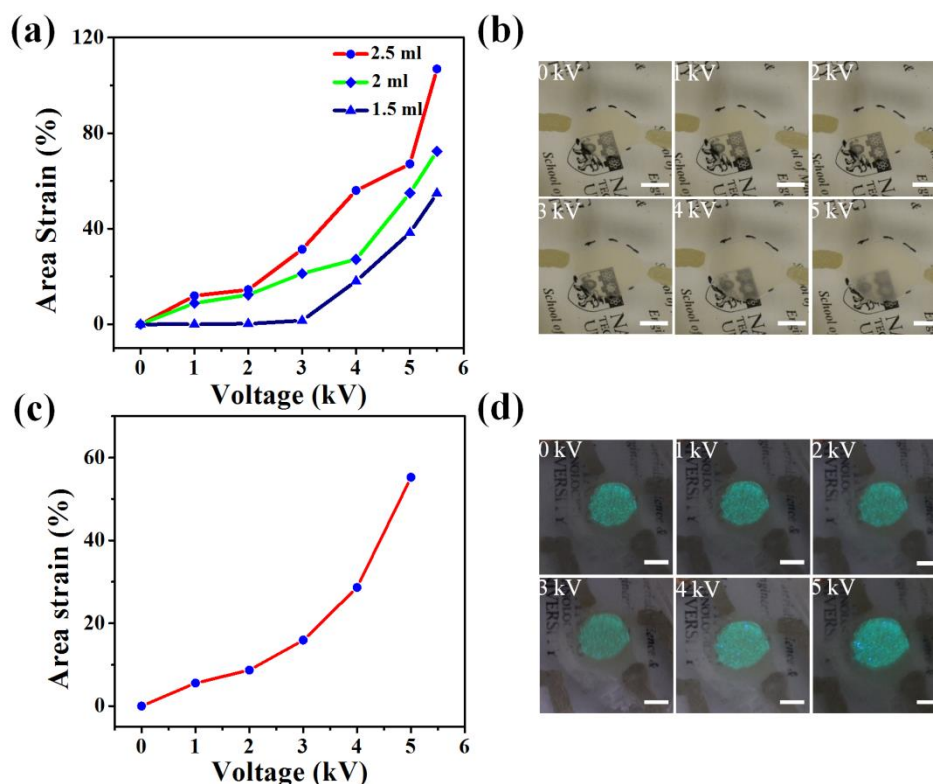


**Figure 5.** (a) Electrical actuation performance test of the DEAs with different amount of AgNWs. (b) Photographs of the DEA under different actuating voltages. (c) Electrical actuation performance of the DEA integrated with stretchable EL device. (d) Photographs of the device under different actuating voltages. Scale bars in b and d are 0.5 cm.

We have demonstrated a stretchable ACEL device which shows excellent mechanical compliant properties with sustained performance under mechanical strain up to 100%. AgNW networks with good transparency and conductivity are used as the stretchable electrodes. Both the top and bottom electrodes are directly embedded into the polymer matrix by subsequent fabrication processes, which virtually ease the device fabrication. Simplicity of the ACEL

device fabrication provides great possibilities for further modifications such as improving the device performance and incorporating other functionalities. Since the active layer is fabricated with ZnS:Cu particles embedded in the PDMS matrix, improvement in the stretchability of the emission layer can be easily achieved by using other host polymers with higher stretchability. Further improvement in the device stretchability will mainly be challenged by developing transparent electrodes which can maintain their conductivity with stretching strains beyond 100%. Taking full advantages of the simple device fabrication procedure, an innovative self-deformable EL device is demonstrated by integrating the stretchable EL devices with DEAs. Compared to conventional EL devices, the self-deformable EL device offers the special feature of dynamic shape display. The soft EL device can achieve ~55% area strain at the actuating voltage of 5 kV. The fabrication procedure and devices developed here will meet wide applications in deformable and stretchable light-emitting devices, bringing new opportunities for soft EL device applications in displays rendering volumetric contents and systems providing interactive user interfaces *etc.* The applications of stretchable ACEL devices in wearable and portable electronics will also not be limited if ACEL materials working under lower voltage (<30 V)<sup>[40-42]</sup> are employed.

## **Experimental Section**

*Fabrication of the stretchable EL devices:* AgNWs were purchased from Seashell Technology with diameters of 120-150 nm and lengths of 20-50  $\mu\text{m}$ . The AgNW solution was diluted into a concentration of 0.3 mg ml<sup>-1</sup> in IPA before use. The AgNW solution was deposited onto a cured PDMS substrate by a spray gun in the fume hood. Due to the fast evaporation rate of IPA, the solution was immediately dried after being deposited onto the substrates without any heating requirement. Pure PDMS was prepared by mixing the base and curing agent (Sylgard 184, Dow Corning) with a weight ratio of 10:1. The liquid mixture was degassed and thermally cured at 60 °C for two hours. ZnS:Cu micro-particles were purchased from Shanghai KPT company.

The ZnS:Cu/PDMS composite was made by mixing the ZnS:Cu powder with the PDMS liquid in a weight ratio of 2:1. Effect of the different ZnS:Cu/PDMS ratio and thickness of the EL layer is studied and discussed in the supporting information [Figure S8](#). The ZnS:Cu/PDMS composite was spun onto the bottom electrode at a spin rate of 2000 rpm for 120 s. The ZnS:Cu/PDMS was thermally cured at 60 °C for two hours.

*Fabrication of the self-deformable EL devices:* The AgNW solution was sprayed onto the prestrained acrylic elastomer films (3M VHB Tape 4910) through a shadow mask. Silver paste was coated at the edges of the AgNW networks as leads to the external electrical circuit. The stretchable EL device was integrated onto the DEAs with the fabrication procedures described above. The ZnS:Cu/PDMS ratio was 1:2 to reduce effective elastic modulus of the emission layer, as large elastic modulus will further hinder actuation performance of the device. The brightness of the EL device will therefore lower compare to the sample prepared with 2:1 ZnS:Cu/PDMS ratio.

*Characterization:* SEM images of the samples were taken using a field-emission SEM (FE-SEM, JSM 7600F). Photoluminescent spectra of the ZnS:Cu/PDMS were measured by a Shimadzu RF-5301PC spectrofluorophotometer. The strain test of the sample was carried out on a home-made stretching stage in room temperature. A Keithley 2400 source meter was used to power the EL devices. Emission from the device was collected by an optical fiber connected to an Acton SP-2300 monochromator. The spectrum was recorded by a Princeton Pixis 100B spectroscopy CCD detector. Luminance was measured by a Konica CS-200 spectroradiometer.

### **Supporting Information**

Supporting Information is available from the Wiley Online Library or from the author.

### **Acknowledgement**

J. Wang and K. Chee acknowledge the scholarships awarded by Nanyang Technological University, Singapore. This work is partly funded by the NTU-A\*STAR Silicon Technologies Centre of Excellence under the program grant No. 112 3510 003, and the Institute of Sports Research.

- [1] S. I. Park, Y. Xiong, R. H. Kim, P. Elvikis, M. Meitl, D. H. Kim, J. Wu, J. Yoon, C. J. Yu, Z. Liu, Y. Huang, K. C. Hwang, P. Ferreira, X. Li, K. Choquette, J. A. Rogers, *Science* **2009**, *325*, 977.
- [2] R. H. Kim, M. H. Bae, D. G. Kim, H. Y. Cheng, B. H. Kim, D. H. Kim, M. Li, J. Wu, F. Du, H. S. Kim, S. Kim, D. Estrada, S. W. Hong, Y. G. Huang, E. Pop, J. A. Rogers, *Nano Lett.* **2011**, *11*, 3881.
- [3] Z. B. Yu, X. F. Niu, Z. T. Liu, Q. B. Pei, *Adv. Mater.* **2011**, *23*, 3989.
- [4] J. J. Liang, L. Li, K. Tong, Z. Ren, W. Hu, X. F. Niu, Y. S. Chen, Q. B. Pei, *ACS Nano* **2014**, *8*, 1590.
- [5] J. J. Liang, L. Li, X. F. Niu, Z. B. Yu, Q. B. Pei, *Nat. Photonics* **2013**, *7*, 817.
- [6] T. Sekitani, H. Nakajima, H. Maeda, T. Fukushima, T. Aida, K. Hata, T. Someya, *Nat. Mater.* **2009**, *8*, 494.
- [7] M. S. White, M. Kaltenbrunner, E. D. Glowacki, K. Gutnichenko, G. Kettlgruber, I. Graz, S. Aazou, C. Ulbricht, D. A. M. Egbe, M. C. Miron, Z. Major, M. C. Scharber, T. Sekitani, T. Someya, S. Bauer, N. S. Sariciftci, *Nat. Photonics* **2013**, *7*, 811.
- [8] D. Leithinger, D. Lakatos, A. DeVincenzi, M. Blackshaw, H. Ishii, in *Proceedings of the 24th annual ACM symposium on User interface software and technology*, ACM, New York, NY, USA **2011**, page 541.
- [9] M. Blackshaw, A. DeVincenzi, D. Lakatos, D. Leithinger, H. Ishii, in *CHI '11 Extended Abstracts on Human Factors in Computing Systems*, ACM, Vancouver, BC, Canada **2011**, page 1237.
- [10] D. Leithinger, S. Follmer, A. Olwal, S. Luescher, A. Hogge, J. Lee, H. Ishii, in *Proceedings of the SIGCHI Conference on Human Factors in Computing Systems*, ACM, Paris, France **2013**, page 1441.

- [11] S. Follmer, D. Leithinger, A. Olwal, A. Hogge, H. Ishii, in *Proceedings of the 26th annual ACM symposium on User interface software and technology*, ACM, St. Andrews, Scotland, United Kingdom **2013**, page 417.
- [12] H. L. Filiatrault, G. C. Porteous, R. S. Carmichael, G. J. E. Davidson, T. B. Carmichael, *Adv. Mater.* **2012**, *24*, 2673.
- [13] S. Kim, J. Byun, S. Choi, D. Kim, T. Kim, S. Chung, Y. Hong, *Adv. Mater.* **2014**, *26*, 3094.
- [14] J. Yoon, S. Y. Hong, Y. Lim, S.-J. Lee, G. Zi, J. S. Ha, *Adv. Mater.* **2014**, *26*, 6580.
- [15] W. Yuan, L. B. Hu, Z. B. Yu, T. L. Lam, J. Biggs, S. M. Ha, D. J. Xi, B. Chen, M. K. Senesky, G. Gruner, Q. B. Pei, *Adv. Mater.* **2008**, *20*, 621.
- [16] R. Pelrine, R. Kornbluh, Q. B. Pei, J. Joseph, *Science* **2000**, *287*, 836.
- [17] G. Kofod, P. Sommer-Larsen, R. Kronbluh, R. Pelrine, *J. Intell. Mater. Syst. Struct.* **2003**, *14*, 787.
- [18] Q. M. Zhang, V. Bharti, X. Zhao, *Science* **1998**, *280*, 2101.
- [19] I. W. Hunter, S. Lafontaine, in *Solid-State Sensor and Actuator Workshop, 1992. 5th Technical Digest., IEEE*, Hilton Head Island, SC, USA **1992**, page 178
- [20] P. Brochu, Q. B. Pei, *Macromol. Rapid Commun.* **2010**, *31*, 10.
- [21] I. Koo, K. Jung, J. Koo, J. D. Nam, Y. Lee, H. R. Choi, in *2006 Ieee International Conference on Robotics and Automation (Icra)*, Orlando, FL, USA **2006**, page 2220.
- [22] M. Matysek, P. Lotz, T. Winterstein, H. F. Schlaak, in *World Haptics 2009: Third Joint Eurohaptics Conference and Symposium on Haptic Interfaces for Virtual Environment and Teleoperator Systems*, Salt Lake City, UT, USA **2009**, page 290.
- [23] C. Keplinger, J. Y. Sun, C. C. Foo, P. Rothemund, G. M. Whitesides, Z. G. Suo, *Science* **2013**, *341*, 984.
- [24] R. Heydt, R. Kornbluh, J. Eckerle, R. Pelrine, in *Smart Structures and Materials 2006: Electroactive Polymer Actuators and Devices (EAPAD)*, San Diego, CA, USA **2006**, page 61681M.

- [25] R. Pelrine, R. D. Kornbluh, Q. Pei, S. Stanford, S. Oh, J. Eckerle, R. J. Full, M. A. Rosenthal, K. Meijer, in *Smart Structures and Materials 2002: Electroactive Polymer Actuators and Devices (EAPAD)*, San Diego, CA, USA **2002**, page 126.
- [26] S. H. Cho, J. Sung, I. Hwang, R. H. Kim, Y. S. Choi, S. S. Jo, T. W. Lee, C. Park, *Adv. Mater.* **2012**, *24*, 4540.
- [27] S. H. Cho, S. S. Jo, I. Hwang, J. Sung, J. Seo, S.-H. Jung, I. Bae, J. R. Choi, H. Cho, T. Lee, J. K. Lee, T.-W. Lee, C. Park, *ACS Nano* **2013**, *7*, 10809.
- [28] J. Sung, Y. S. Choi, S. J. Kang, S. H. Cho, T.-W. Lee, C. Park, *Nano Lett.* **2011**, *11*, 966.
- [29] V. Wood, J. E. Halpert, M. J. Panzer, M. G. Bawendi, V. Bulovic, *Nano Lett.* **2009**, *9*, 2367.
- [30] Z.-g. Wang, Y.-f. Chen, P.-j. Li, X. Hao, J.-b. Liu, R. Huang, Y.-r. Li, *ACS Nano* **2011**, *5*, 7149.
- [31] J. N. Lee, C. Park, G. M. Whitesides, *Anal. Chem.* **2003**, *75*, 6544.
- [32] C. Y. Yan, J. X. Wang, X. Wang, W. B. Kang, M. Q. Cui, C. Y. Foo, P. S. Lee, *Adv. Mater.* **2014**, *26*, 943.
- [33] T. Akter, W. S. Kim, *ACS Appl. Mater. Interfaces* **2012**, *4*, 1855.
- [34] J. Wang, C. Yan, W. Kang, P. S. Lee, *Nanoscale* **2014**, *6*, 10734.
- [35] W. L. Hu, X. F. Niu, L. Li, S. R. Yun, Z. B. Yu, Q. B. Pei, *Nanotechnology* **2012**, *23*, 344002.
- [36] M. A. Eddings, M. A. Johnson, B. K. Gale, *J. Micromech. Microeng.* **2008**, *18*, 067001.
- [37] D. R. Vij, *Handbook of electroluminescent materials*, Institute of Physics Publishing, Kurukshetra, India **2004**.
- [38] P. Z. Philips, *Research Reports* **1956**, *11*, 417.
- [39] I. T. Steinberger, V. Bar, E. Alexander, *Phys. Rev.* **1961**, *121*, 118.
- [40] J. Sung, Y. S. Choi, S. J. Kang, S. H. Cho, T.-W. Lee, C. Park, *Nano Lett.* **2011**, *11*, 966.

[41] S. H. Cho, J. Sung, I. Hwang, R. H. Kim, Y. S. Choi, S. S. Jo, T. W. Lee, C. Park, *Adv. Mater.* **2012**, *24*, 4540.

[42] S. H. Cho, S. S. Jo, I. Hwang, J. Sung, J. Seo, S.-H. Jung, I. Bae, J. R. Choi, H. Cho, T. Lee, J. K. Lee, T.-W. Lee, C. Park, *ACS Nano* **2013**, *7*, 10809.

**Table of Contents Entry**

A highly stretchable light-emitting device based on alternating-current EL (ACEL) material is fabricated by a simple and all-solution processible method. The ACEL device shows stable emission performance with strain up to 100% which can be repetitively stretched to 80% strain. Furthermore, a novel self-deformable EL device which can be electrically driven into dynamic shapes is demonstrated by integrating the device with dielectric elastomer actuators (DEAs).

**Keywords:**

Stretchable light-emitting devices, self-deformable, alternating current electroluminescent, actuator, nanowires

**Authors:**

Jiangxin Wang, Chaoyi Yan, Kenji Jianzhi Chee, and Pooi See Lee \*

**Title:**

**Highly stretchable and self-deformable alternating current electroluminescent devices**

**TOC Image:**

